⌘ *Author's Choice*

THE JOURNAL OF BIOLOGICAL CHEMISTRY VOL. 286, NO. 49, pp. 42704–42714, December 9, 2011

The *Escherichia coli* Clamp Loader Can Actively Pry Open the β-Sliding Clamp*[S]

Received for publication, June 3, 2011, and in revised form, September 30, 2011 Published, JBC Papers in Press, October 4, 2011, DOI 10.1074/jbc.M111.268169

Christopher O. Paschall[‡], Jennifer A. Thompson[‡], Melissa R. Marzahn[‡], Ankita Chiraniya[‡], Jaclyn N. Hayner[‡], Mike O'Donnell[§], Arthur H. Robbins[‡], Robert McKenna[‡], and Linda B. Bloom[‡1]

From the [‡]Department of Biochemistry and Molecular Biology, University of Florida, Gainesville, Florida 32610-0245 and the [§]Howard Hughes Medical Institute and Rockefeller University, New York, New York 10021

Clamp loaders load ring-shaped sliding clamps onto DNA. Once loaded onto DNA, sliding clamps bind to DNA polymerases to increase the processivity of DNA synthesis. To load clamps onto DNA, an open clamp loader-clamp complex must form. An unresolved question is whether clamp loaders capture clamps that have transiently opened or whether clamp loaders bind closed clamps and actively open clamps. A simple fluorescence-based clamp opening assay was developed to address this question and to determine how ATP binding contributes to clamp opening. A direct comparison of real time binding and opening reactions revealed that the *Escherichia coli* γ complex binds β first and then opens the clamp. Mutation of conserved "arginine fingers" in the γ complex that interact with bound ATP decreased clamp opening activity showing that arginine fingers make an important contribution to the ATP-induced conformational changes that allow the clamp loader to pry open the clamp.

DNA polymerase processivity factors, a sliding clamp and clamp loader, are essential for DNA replication in all domains of life. DNA is synthesized by DNA polymerases, but without these processivity factors DNA polymerases would frequently dissociate from the template being copied leading to relatively inefficient DNA replication. Clamp loaders load sliding clamps onto DNA at sites where DNA polymerases will begin synthesis. Sliding clamps bind to DNA polymerases and, at the same time, encircle the DNA template to greatly decrease dissociation of the DNA polymerase from the template.

Many structural features of sliding clamps and clamp loaders are also conserved in all domains of life. Sliding clamps are ring-shaped complexes of crescent-shaped monomers. The overall structure of sliding clamps is strikingly similar even though they may differ in the number of monomers that make-up a six-domain ring; some are dimers (each with three domains), and others are trimers (each with two domains). The *Escherichia coli* β sliding clamp is an example of a dimeric ring, whereas proliferating cell nuclear antigen (PCNA)[2] in eukaryotes and bacteriophage T4 gp45 sliding clamps are trimers. Crystal structures of each of these sliding clamps have been determined, and all exhibited a closed ring form (1–4). When loaded onto circular DNA templates, the β-clamp and PCNA remain stably bound to DNA with half-lives of more than an hour and about a half-hour, respectively, supporting the idea that these clamps exist predominantly as closed rings in solution (5, 6). On the other hand, fluorescence resonance energy transfer studies indicate that a population of open gp45 clamps is present in solution (7, 8).

Clamp loaders catalyze the mechanical assembly of these ring-shaped sliding clamps onto DNA and are members of the AAA+ family of ATPases (for review, see Refs. 9–11). ATP binding and hydrolysis drive conformational changes in the clamp loaders that modulate the affinity of the clamp loaders for the clamp and DNA. This affinity modulation gives the clamp loaders a high affinity for the clamp and DNA to bring these macromolecules together during the first stage of the clamp loading reaction cycle, and then a reduction in affinity allows the clamp loaders to release the clamps on DNA during the second stage of the reaction.

Clamps must adopt an open conformation to be loaded onto DNA by clamp loaders. The question is, how does an open clamp loader-clamp complex form. One possibility is that clamp loaders have a high affinity for open clamps and preferentially bind clamps existing in an open conformation in solution. Alternatively, clamp loaders may bind closed clamps and actively pry clamps open. In the T4 system, a population of open clamps is present in solution, and the clamp loader binds open clamps and chaperones them to DNA (12, 13). The T4 clamp loader can also load clamps on DNA in reactions in which the clamp loader first binds to DNA and then captures a clamp (14). Given the structure of a clamp loader-DNA complex (15), bound DNA would sterically prohibit the T4 clamp loader from binding closed clamps before opening them, supporting the model that the T4 clamp loader preferentially binds open clamps. The mechanism of clamp opening has not been determined for the *E. coli* β-clamp or eukaryotic PCNA. It is possible that ATP binding gives the *E. coli* γ complex and eukaryotic replication factor C (RFC) a high affinity for open

* This work was supported, in whole or in part, by National Institutes of Health Grants GM055596 and GM082849 (to L. B. B.) and GM038839 (to M. O. D.).

[S] The on-line version of this article (available at http://www.jbc.org) contains supplemental Figs. 1 and 2.

⌘ *Author's Choice*—Final version full access.

The atomic coordinates and structure factors (code 3PWE) have been deposited in the Protein Data Bank, Research Collaboratory for Structural Bioinformatics, Rutgers University, New Brunswick, NJ (http://www.rcsb.org/).

[1] To whom correspondence should be addressed: 1600 SW Archer Rd., JHMHC R3-234, Dept. of Biochemistry and Molecular Biology, University of Florida, Gainesville, FL 32610-0245. Tel.: 352-392-8708; Fax: 352-392-6511; E-mail: lbloom@ufl.edu.

[2] The abbreviations used are: PCNA, proliferating cell nuclear antigen; AF488, Alexa Fluor 488; β-AF488$_2$, β double-mutant (R103C/I305C) labeled with AF488; PY, pyrene; RFC, replication factor C; ATPγS, adenosine 5′-*O*-(thiotriphosphate); r.m.s., root mean square.

clamps and that, like the T4 clamp loader, these clamp loaders simply capture clamps that have transiently opened. Given the stability of the β-clamp and PCNA relative to gp45 (6), it may be that the mechanism of clamp opening by γ complex and RFC differ from that for the T4 clamp loader. The γ complex and RFC may bind closed clamps and actively open them. To determine which opening mechanism is operative, a clamp opening assay was developed to measure the rate of clamp opening relative to the rate of clamp binding by the *E. coli* γ complex.

EXPERIMENTAL PROCEDURES

Buffers and Reagents—Assay buffer contains 20 mM Tris-HCl, pH 7.5, 50 mM sodium chloride, 8 mM magnesium chloride, 2 mM DTT, and 4% glycerol. Storage buffer for β clamp contains 20 mM Tris-HCl, pH 7.5, 0.5 mM EDTA, 2 mM DTT, and 10% glycerol. Storage buffer for γ complex is the same except for the inclusion of 50 mM sodium chloride.

Proteins—Individual γ complex subunits were purified, and the γ complex was reconstituted as described previously (16–20). Complexes containing arginine finger mutations were prepared by in the O'Donnell laboratory as described (21). Pyrene-labeled β was prepared as described (22).

β Mutants for Clamp Opening Assays—Mutations were introduced into the *dnaN* coding sequence by site-directed mutagenesis to make β mutants that could be singly-labeled R103C/C260S/C333S and I305C/C260S/C333S or doubly-labeled R103C/I305C/C260S/C333S with Alexa Fluor 488 (AF488). The β mutants were expressed in *E. coli* BL21(DE3) cells and purified following published procedures (16, 23). Purified β mutants were labeled with Alexa Fluor 488 C5-maleimide (Invitrogen) by incubating a solution of β and AF488, typically containing 60 μM β and 1.67 mM AF488 in 50 mM potassium phosphate buffer, pH 7.4, with 1 mM Tris(2-carboxyethyl)phosphine, for 2 h at room temperature and overnight at 4 °C. Excess fluorophore was removed by gel filtration on Bio-Gel P6DG (Bio-Rad) followed by ion exchange chromatography on a HiTrap Q-Sepharose column (GE Healthcare). The fraction of labeled β was calculated from the protein concentration, measured using a Bradford-type assay (Bio-Rad) with wt β standards. The AF488 concentration was calculated from the absorbance of AF488 measured when the protein was denatured in buffer containing 8 M guanidine hydrochloride and 67 mM sodium phosphate at pH 6. An extinction coefficient for AF488 of 73,000 $M^{-1}cm^{-1}$ at 493 nm provided by the supplier (Invitrogen) was used. Based on these calculations, labeling efficiencies were 100–110%. We believe this number is artificially high due to changes in the AF488 extinction coefficient on conjugation to β or to the effects of the fluorophores on determining the protein concentration.

X-ray Crystallography—Crystals were grown using the hanging drop vapor diffusion method at room temperature. Purified protein, β-$AF488_2$ (1.8 mg/ml), was mixed with an equal volume of the precipitant solution (100 mM MES, pH 6.0, 125 mM calcium chloride, 30% PEG 400) for a final volume of 4 μl (24). The drops were equilibrated against 0.5 ml of precipitant solution, and crystals were observed after about 3 days. The crystals were quick-dipped into a cryoprotectant solution of precipitant solution with 25% (v/v) glycerol before being flash-cooled to 100 K for data collection. At the beginning of data collection, crystals were bright green due to AF488, but by the end the crystals were colorless, indicating that the fluorophore was bleached during data collection.

Diffraction data were collected in-house using a Rigaku RU-H3R rotating anode equipped with VariMax HR optic and R-AXIS IV++ image plate detector. Data were indexed and scaled using *HKL2000* (25), and the structure was solved using molecular replacement (PDB ID 1MMI (24)). Refinement was initiated using PHENIX (26) and changes to the model between rounds of refinement were made using Coot (27). PROCHECK was used to check the final geometry of the model (28). Data collection and refinement statistics are given in Table 1.

Fluorescence Measurements in Equilibrium Binding and Opening Experiments—AF488 was excited at 495 nm, emission spectra were measured using a 3 nm bandpass, and relative intensity values at 517 nm were calculated. Pyrene was excited at 345 nm, emission spectra were recorded using a 3-nm bandpass, and relative intensities at 375 nm were calculated. Buffer background signals were subtracted from spectra, and relative intensities were calculated by dividing intensities for solutions containing γ complex by the intensity for free β. The relative intensity of samples containing no γ complex was set to 1. Three independent experiments were done for each titration. K_d values for γ complex binding β-$AF488_2$ (Fig. 3*A*) were calculated for each experiment using Equation 1, where β_o is the total concentration of β, γ_o is the total concentration of γ complex, and I_{max} and I_{min} are the maximum and minimum intensities, respectively.

$$I_{obs} = \left(\frac{K_d + \beta_o + \gamma_o - \sqrt{(K_d + \beta_o + \gamma_o)^2 - 4\beta_o\gamma_o}}{2\beta_o} \right) \times (I_{max} - I_{min}) + I_{min} \quad \text{(Eq. 1)}$$

In competition binding experiments, a solution of γ complex was added to a solution of β-$AF488_2$ and unlabeled β. The concentration of β-$AF488_2$ was held constant at 20 nM, and the concentration of unlabeled β was varied. The data were fit to Equation 2 to calculate K_d values for unlabeled β, where β_{AF} is the β-$AF488_2$ concentration, β_o is the total (labeled and unlabeled) β concentration, and other terms are defined as in Equation 1.

$$I_{obs} = \left(\frac{\beta_{AF}}{\beta_o} \right) \left(\frac{K_d + \beta_o + \gamma_o - \sqrt{(K_d + \beta_o + \gamma_o)^2 - 4\beta_o\gamma_o}}{2\beta_o} \right) \times (I_{max} - I_{min}) + I_{min} \quad \text{(Eq. 2)}$$

Stopped-flow Clamp Closing Assay—Sequential mix experiments were performed in which a syringe containing γ complex was mixed with a syringe containing β-$AF488_2$ and ATP. After 4 s this solution was then mixed with a syringe containing an excess of unlabeled β as a chase with and without DNA. The reaction was excited at 490 nm using a 3.7-nm bandpass, and emission was measured using a 515-nm cut-on filter. Measurements were collected for 60 s at 3-ms intervals. The reaction containing DNA was fit to a single exponential decay. The reaction lacking DNA has a small but reproducible increase in fluo-

rescence at early times. This reaction was fit to the sum of an exponential rise and an exponential decay. Amplitudes and rates were 0.055 and 22 s^{-1}, respectively, for the small rise and 0.35 and 0.027 s^{-1}, respectively, for the decay.

Stopped-flow Clamp Binding and Opening Assays—Single-mix experiments were done in which γ complex and ATP present in one syringe were added to labeled β and ATP from a second syringe. All reactions were done in assay buffer, and protein concentrations reported are final concentrations after mixing the contents of the two syringes. Time course data were collected for 35 s using a split time base in which 5000 data points were collected at 1-ms intervals followed by 10,000 data points at 3-ms intervals. AF488 was excited at 490 nm using a 3.7-nm bandpass, and emission was measured using a 515-nm cut-on filter. Pyrene was excited at 345 nm using a 3.7-nm bandpass, and emission was measured using a 365-nm cut-on filter. In experiments comparing the kinetics of clamp binding to clamp opening, intensities relative to the starting free-labeled β concentrations are plotted. For clamp opening reactions done as a function of γ complex concentration, the increase in AF488 fluorescence for clamp opening reactions was normalized from 0 to 1. The data sets were globally fit using GraphPad Prism to Equation 3 in which a represents the amplitude of the phases, k_{obs} is the observed rate constant, t is time, and c is a constant.

$$y = a_{fast}(1 - e^{-k_{obs,fast}t}) + a_{slow}(1 - e^{-k_{obs,slow}t}) + c \quad \text{(Eq. 3)}$$

A constant was added because the data are not simple exponentials but contain a small lag at early times, and inclusion of the constant gives a better fit to the initial rapid increase in fluorescence. The amplitudes for the rapid and slow phases were constrained to be the same for each time course. Increase in k_{obs} values as a function of γ complex concentration (Fig. 7*B*) were fit to Equation 4 to calculate a maximal rate, k_{max}, where K_{dc} is the dissociation constant for forming the closed complex.

$$k_{obs} = \left(\frac{K_{dc} + \beta_o + \gamma_o - \sqrt{(K_{dc} + \beta_o + \gamma_o)^2 - 4\beta_o\gamma_o}}{2\beta_o}\right) \times k_{max} \quad \text{(Eq. 4)}$$

RESULTS

β Mutant for Clamp Opening Assay—Two amino acid residues, Arg-103 and Ile-305, were converted to Cys to provide sites for labeling, and two surface cysteines, Cys-260 and Cys-333, were converted to Ser to allow selective labeling of Cys-103 and Cys-305. The purified β mutant was labeled with AF488 in the presence of a reducing agent to prevent disulfide bond formation between the closely spaced cysteines. Cys-103 and Cys-305 are juxtaposed on opposite sides of the interfaces between the two monomers in the β dimer (Fig. 1*A*). The AF488-labeled β mutant (β-$AF488_2$) was crystallized, and the structure was determined (crystals diffracted to 2.2 Å resolution) to verify that these four mutations do not adversely affect the structure of the clamp particularly at the interface. The structure of β-$AF488_2$ (*blue*, PDB ID 3PWE) was overlaid on a structure of wild-type β (*orange*, PDB ID 1MMI (24)) that crystallized in the same space group and that diffracted to 1.85Å resolution.

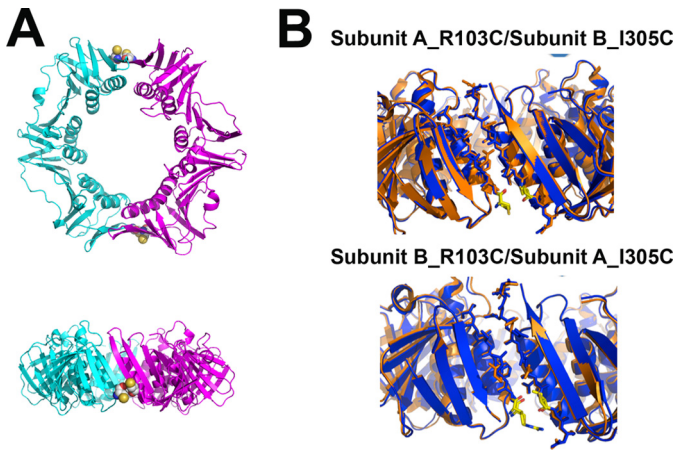

FIGURE 1. **Structure of the β mutant used in the clamp opening assay.** *A*, the ribbon diagram in the *upper panel* shows a top view of β from the face to which the γ complex binds. One monomer is colored in *cyan*, and the other is in *magenta*. Amino acid residues Cys-103 and Cys-305 are shown as *spheres* colored by atoms with carbon in *white*, nitrogen in *blue*, oxygen in *red*, and sulfur in *yellow*. The *lower panel* shows an edge view of the same structure in which the γ complex would bind with the top face of the clamp. *B*, an overlay of structures of β-wt (*orange*, PDB ID 1MMI (24)) and the β-$AF488_2$ (*blue*, PDB ID 3PWE) are shown in an edge view. The β strands on either side of the monomer interface are shown as sticks with wild-type Arg-103 and Ile-305 and mutant Cys-103 and Cys-305 colored by atoms with carbon in *yellow*, nitrogen in *blue*, oxygen in *red*, and sulfur in *orange*. The *upper panel* shows one interface with r.m.s. deviation values for the backbone between the wild-type and mutant structures of 0.11 Å for residues 103–109 in the A subunit and 0.14 Å for residues 298–307 in the B subunit. The *lower panel* shows the opposite dimer interface with r.m.s. deviation values of 0.06 Å for residues 103–109 in the B subunit and 0.29 Å for residues 298–307 in the A subunit. r.m.s. deviations were calculated using Coot (27).

The overall r.m.s. deviation in the peptide backbone between the two structures was 0.44 Å. Edge views of the clamp focusing on the β strands at the dimer interfaces containing the R103C and I305C mutations (Fig. 1*B*) show that the overall structure at the dimer interface is the same in the wild-type and mutant clamps, within the resolution limits of the crystal structures (Table 1). In the refined structure, residual density was observed in the $F_o - F_c$ electron density map, in close proximately to Cys-103 and Cys-305 in β-$AF488_2$, which we attribute to the presence of the AF488 fluorophore (supplemental Fig. 1). However, this density was diffuse and ill-defined, and therefore was not modeled as the fluorophore molecule. The main contribution to the incomplete density is likely due to conformational mobility of AF488. The AF488 maleimide derivative contains a five-carbon atom linker between the maleimide and fluorophore moieties. Although labeling reactions were efficient, incomplete labeling of all four cysteine residues may also contribute.

A Fluorescence Intensity-based Assay to Measure β-Clamp Opening—A clamp-opening assay was developed to measure the relative timing of clamp opening and closing during the course of the clamp-loading reaction catalyzed by the *E. coli* γ complex. The assay takes advantage of the property that two fluorophores within close proximity will self-quench. The distance between α-carbon atoms in Cys-103 and Cys-305 residues is 5.4 Å based on the crystal structure. This double mutant contains two Cys residues per β monomer, both of which can be labeled with AF488 to form β-$AF488_2$. As a control, single mutants were also constructed that contained only the Arg-103

TABLE 1
X-ray crystallographic data collection and refinement statistics
Values in parentheses are for the highest resolution bin.

Data collection	
Wavelength (Å)	1.5418
Space group	$P2_1$
Unit cell parameters (Å, °)	$a = 79.8$ $b = 67.4$ $c = 80.7$, $\beta = 114.2$
Molecules in asymmetric unit	2
Solvent content (%)	49.6
Resolution (Å)	28.5-2.2 (2.28-2.2)
Number of unique reflections	39,772
Completeness (%)	99.6 (100)
Redundancy	3.1 (3.1)
Refinement	
R_{merge} [a] (%)	9.9 (47.9)
$I/\sigma(I)$	11.2 (2.2)
Number of reflections used for R_{cryst}	37,766
Number of reflections used for R_{free}	2,006
R_{cryst} [b] (%)/R_{free} [c] (%)	20.4/24.5
r.m.s. deviations	
Bond lengths (Å)	0.008
Bond angles (°)	0.971
Ramachandran statistics (%)	
Favored	92.9
Allowed	6.4
Generously allowed	0.6
Outliers	0.0
Number of protein atoms	5,691
Number of solvent atoms	335
Average B factors (Å^2)	
Main chain	32.7
Side chain	42.2
Solvent	33.9

[a] $R_{merge} = \Sigma|I - \langle I\rangle|/\Sigma\langle I\rangle \times 100$.
[b] $R_{cryst} = \Sigma||F_o| - |F_c||/\Sigma|F_{obs}| \times 100$.
[c] R_{free} is calculated in the same manner as R_{cryst} except that it uses 5% of the reflection data omitted from refinement.

to Cys or Ile-305 to Cys mutation in the C260S and C333S background, and the single mutants were labeled with AF488. The absolute fluorescence intensity of a 10 nM solution of the double mutant was about 3-fold less than the single mutants at the same concentration (Fig. 2*A*). Given that the double mutant should give about twice the fluorescence of a single mutant if the fluorophores were not interacting, each pair of fluorophores in the double mutant is most likely self-quenching.

Experiments were done that should physically separate the fluorophores in the double mutant to confirm that the difference in fluorescence between the double and single mutants was due to self-quenching in the double mutant. All three clamps were denatured by the addition of SDS to a final concentration of 5%. Denaturation of the double mutant increased the fluorescence intensity of AF488 by a factor of about 6 (Fig. 2*B*), whereas denaturation of the single mutants gave a much smaller increase in fluorescence, about a 1.6-fold increase for the R103C mutant and 1.1-fold increase for the I305C mutant (Fig. 2*C*). The large increase in AF488 fluorescence in the double mutant is due to the relief of self-quenching, and the small change in the single mutants is likely an environmental effect of the SDS and/or protein unfolding.

The addition of the γ complex to all three clamps in the presence of ATP should form an open clamp loader-clamp complex (29). When the γ complex was added to the double mutant, the fluorescence of AF488 increased by a factor of 2.5 (Fig. 2*D*), whereas the addition of the γ complex to the single mutants had no effect on the fluorescence of AF488 (Fig. 2*E*). Interestingly, AF488 fluorescence in the open clamp loader-clamp complex is about half that for the denatured clamp, which is consistent with the idea that only one interface of the dimeric β ring is opened by the clamp loader so the quench is relieved in only one pair of fluorophores (compare the maximal intensity of the black spectrum in Fig. 2*D* to that in Fig. 2*B*). Together, these results demonstrate that AF488 is self-quenched in the double mutant when the clamp is closed, and the fluorescence increases when the fluorophores are physically separated by clamp opening or protein denaturation.

The efficiency of labeling the double mutant varies from preparation to preparation. Higher labeling efficiencies give a greater quench and, thus, a larger increase on opening. Because of differences in the efficiency of labeling, each preparation of protein has its own effective quantum yield for the change, and this must be taken into account when calculating the fraction of open clamps. As long as this difference is considered, equilibrium constants and kinetic constants determined using different preparations are the same.

β-AF488$_2$-γ Complex Binding—Equilibrium binding interactions between the γ complex and β were measured to determine whether the site-directed mutations and/or the fluorophores in β-AF488$_2$ adversely affect protein-protein interactions. The dissociation constant was determined by measuring the fluorescence of AF488 in solutions containing 10 nM β-AF488$_2$ and increasing concentrations of the γ complex in the presence of 0.5 mM ATP. The fluorescence of AF488 increased with the concentration of γ complex in the manner expected for an equilibrium binding reaction (Fig. 3*A*). A dissociation constant, K_d, of 3.3 ± 0.2 nM was calculated from these data, which is in agreement with the K_d value of 3.2 nM previously measured for the wild-type unlabeled proteins (30).

To confirm that β-AF488$_2$ binds γ complex with the same affinity as unlabeled wild-type β (β-wt), a competition binding assay was performed. In this assay γ complex was added to a solution containing a constant concentration of β-AF488$_2$ and increasing concentrations of β-wt. Final concentrations were 20 nM γ complex, 20 nM β-AF488$_2$, and 0–320 nM β-wt. The AF488 fluorescence decreased with increasing concentrations of β-wt as the unlabeled clamp competed for binding to γ complex (Fig. 3*B*). These competition data were fit to Equation 2 ("Experimental Procedures") to calculate a K_d value for γ complex binding β-wt. This equation takes into account the increase in the total fraction of γ complex bound by β, either β-AF488$_2$ or β-wt, that occurs when the total concentration of β increases (Fig. 3*B*, *black line*). At the start of the titration, 0 nM unlabeled β, about two-thirds of the γ complex is bound based on the K_d value of 3.3 nM. A K_d value of 3.2 ± 0.4 nM was calculated for β-wt binding confirming that γ complex binds β-AF488$_2$ with the same affinity as wild-type β.

Loading the β-AF488$_2$ Clamp—Clamp loading reactions were done to show that the β-AF488$_2$ clamp could be productively loaded onto DNA and that the fluorescence of AF488 decreased when the clamp was released onto DNA and closed. In these reactions, the clamp loader was preincubated with the clamp and ATP to form an open clamp loader-clamp complex before adding DNA to trigger the loading reaction. An excess of unlabeled β was added to limit the reaction to a single-turnover. The time course for the reaction shows a decrease in fluores-

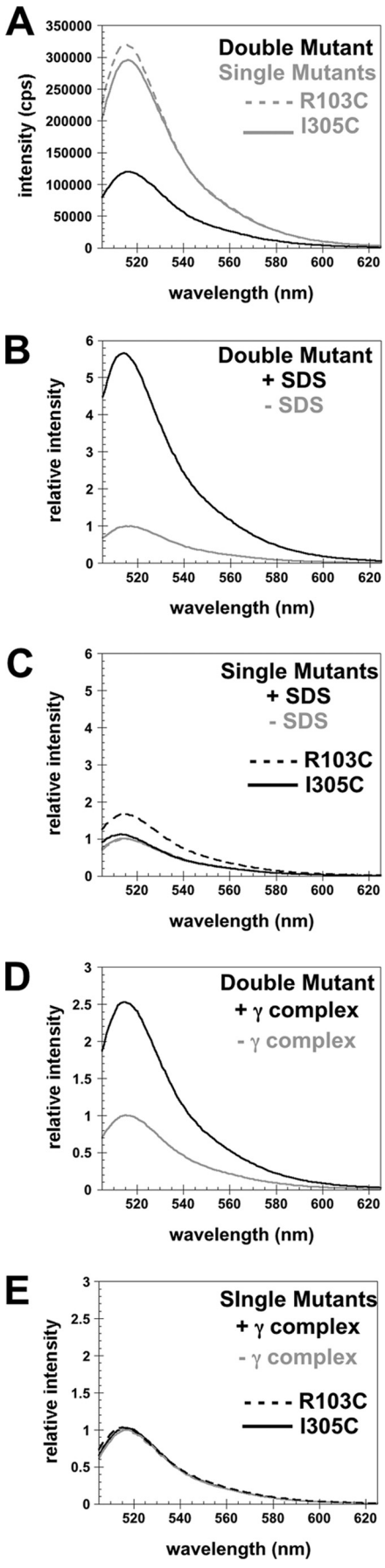

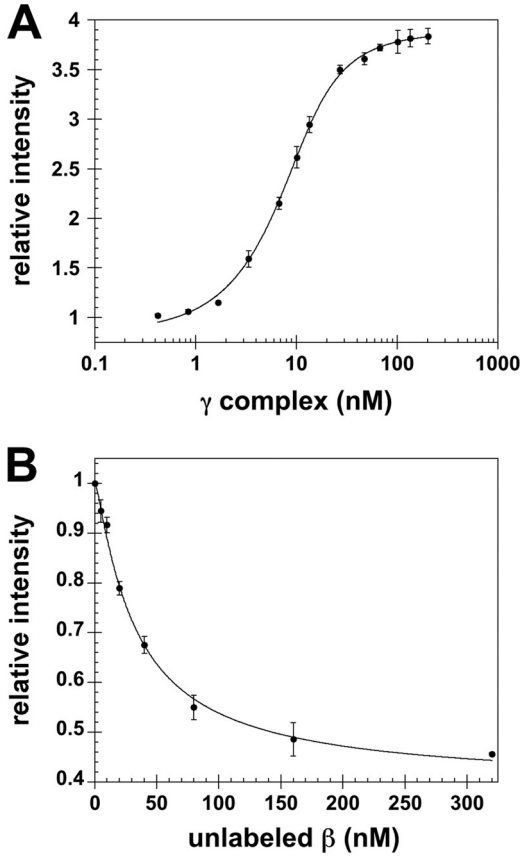

FIGURE 3. **Equilibrium binding of γ complex to β.** *A*, the relative intensity of AF488 at 517 nm is plotted as a function of γ complex concentration for solutions containing 10 nM β-AF488$_2$ and 0.5 mM ATP. Data from individual experiments were fit Equation 1 ("Experimental Procedures") to calculate an average dissociation constant, K_d, of 3.3 ± 0.2 nM. *B*, competition binding of γ complex to wt unlabeled β *versus* β-AF488$_2$ was measured in assays containing 20 nM γ complex, 20 nM β-AF488$_2$, 0.5 mM ATP, and increasing concentrations of unlabeled β-wt. The relative fluorescence of AF488 is plotted as a function of the concentration of the unlabeled β competitor. Data were fit to Equation 2 ("Experimental Procedures") to calculate an average K_d value of 3.2 ± 0.4 nM for β-wt.

cence as a function of time as expected (Fig. 4*A*). There are two possible mechanisms by which the clamp can disengage from the clamp loader during this reaction. The first is by a productive clamp-loading reaction, and the second is by a passive dissociation reaction in which the clamp simply dissociates from the clamp loader. To show that we can distinguish between these two possibilities, clamp closing was measured in a reaction without DNA in which the clamp can only disengage from the clamp loader by a passive dissociation mechanism.

FIGURE 2. **A comparison of β single and double mutants shows that physical separation of the two AF488 fluorophores in the double mutant relieves self-quenching.** *A*, shown are emission spectra of 10 nM solutions of the AF488-labeled single mutants (R103C, *gray dashed line* and I305C, *gray solid line*) and double mutant (R103C/I305C, *black line*) in assay buffer. *B* and *C*, show emission spectra of 10 nM solutions of the double and single mutants, respectively, in solutions of assay buffer with (*black trace*) and without (*gray trace*) 5% SDS. The R103C single mutant is shown in *dashed lines*, and I305C single mutant is shown in *solid lines*. *D* and *E* show emission spectra of 10 nM solutions of the double and single mutants, respectively, in solutions containing 0.5 mM ATP in assay buffer with (*black trace*) and without (*gray trace*) 150 nM γ complex. The R103C single mutant is shown in *dashed lines*, and I305C single mutant is shown in *solid lines*. All spectra were recorded using a 495-nm excitation wavelength and a 3-nm bandpass. Assay buffer contains 20 mM Tris-HCl, pH 7.5, 50 mM NaCl, and 8 mM $MgCl_2$.

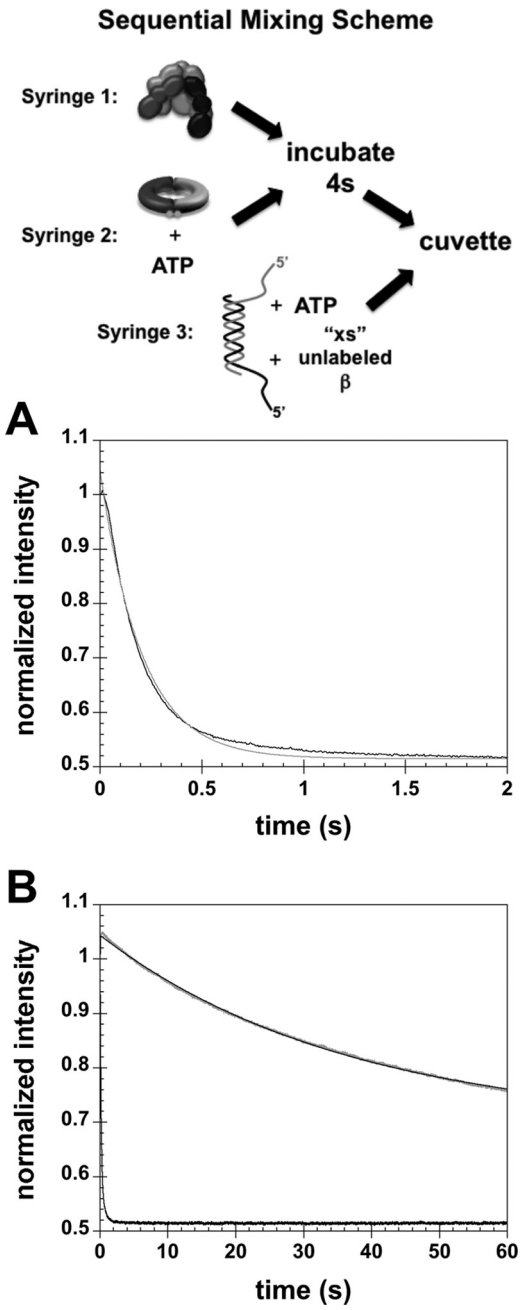

FIGURE 4. **Clamp closing in real time by active clamp loading and passive dissociation reactions.** *A*, the γ complex was preincubated with β and ATP for 4 s before adding a solution of DNA, ATP, and a 10-fold excess ("*xs*") of unlabeled β. The decrease in fluorescence that occurred when the clamp was loaded onto DNA and closed was measured as a function of time. The *solid gray line* through the trace is a single exponential fit to the data to calculate an observed closing rate of 4.9 s^{-1}. The DNA substrate used in this experiment was a 60/60-mer duplex annealed to create two 3′ recessed ends with 30-nucleotide 5′ single-stranded DNA overhangs. *B*, clamp closing that occurs when the clamp "passively" dissociates from the clamp loader was measured under identical reaction conditions except that DNA was omitted. The passive dissociation reaction (*upper gray trace*) was fit by exponentials to calculate a closing rate of 0.027 s^{-1}. For comparison, the reaction with DNA (*lower black trace*) is plotted on the same time scale. Final concentrations were 20 nM γ complex, 20 nM β-AF488$_2$, 0.5 mM ATP, 200 nM unlabeled β, and 40 nM DNA when present.

This reaction was done under identical conditions except for the omission of DNA (Fig. 4*B*). The rate of decrease in AF488 fluorescence for the passive dissociation reaction is about 200-fold slower, 0.027 s^{-1}, than that for the clamp loading reaction in the presence of DNA, 4.9 s^{-1}. Based on this difference in kinetics, the faster reaction is the result of active loading of the clamp on DNA.

ATP Requirements for Clamp Opening—Earlier work has established that ATP binding to the γ complex promotes a conformational change that gives the γ complex a high affinity for the clamp (29, 30) to form an open β-γ complex (29, 31). The γ complex also binds β in the absence of ATP but with much lower, 100–1000-fold, affinity (30, 32). The weaker binding could be attributed to 1) a small fraction of γ complex that is able to productively bind β in the absence of ATP or 2) formation of a clamp loader-clamp complex in which β is closed. To determine the nature of this weaker ATP-independent binding interaction, a comparison of β binding and β opening was made using two separate fluorescence-based assays. Binding was measured using a fluorescence intensity-based assay in which β was labeled with pyrene (PY) on the surface to which the γ complex binds (22). When the γ complex binds PY-labeled β (β-PY), the intensity of PY increases. Opening of β was measured in the relief of self-quench assay using β-AF488$_2$. Binding/opening titrations were done in parallel using increasing concentrations of γ complex. A two-step procedure was used in which the γ complex was added to the clamps first to measure binding/opening in the absence of ATP, and then ATP (0.5 mM final concentration) was added to measure binding/opening in the presence of ATP. In the β-PY binding assay (Fig. 5*A*), the increase in PY fluorescence due to binding occurs at lower γ complex concentrations in the presence of ATP (*gray bars*) than in the absence of ATP (*black bars*) as expected due to weaker ATP independent binding. Comparison of these binding data to the opening data (Fig. 5*B*) shows that in the presence of ATP (*gray bars*), both β binding and opening occur over the same range of γ complex concentrations. In contrast, in the absence of ATP (*black bars*), β opening does not occur at γ complex concentrations where β binding is observed. These results demonstrate that in the absence of ATP, closed clamp loader-clamp complexes are present, whereas in the presence of ATP open clamp loader-clamp complexes are present.

A single γ complex subunit, the δ subunit, can catalyze the removal of β clamps from circular DNA molecules (5, 29, 33). Using this relief of self-quench assay, clamp opening by the δ subunit alone was not detectable at concentrations up to 6 μM δ (data not shown). This is consistent with experiments showing that an internal surface of the β dimer interface could be labeled in the presence of γ complex but not when δ alone was added (29). Although the δ subunit can transiently open clamps to unload clamps from circular DNA, these data show that a stable open β-δ complex does not form in solution.

Arginine Finger Mutants of γ Complex Are Defective in Clamp Opening—In the γ complex and other AAA+ family members, subunits are arranged such that each of the ATP binding sites is located at a subunit-subunit interface, and a conserved arginine residue or Arg finger (for review, see Ref. 34), extends from one subunit to the neighboring ATP site. These Arg fingers have been shown to be important for catalyzing ATP hydrolysis (21, 35) and also in sensing the γ-phosphate of bound ATP (32, 36). The γ complex contains three ATP

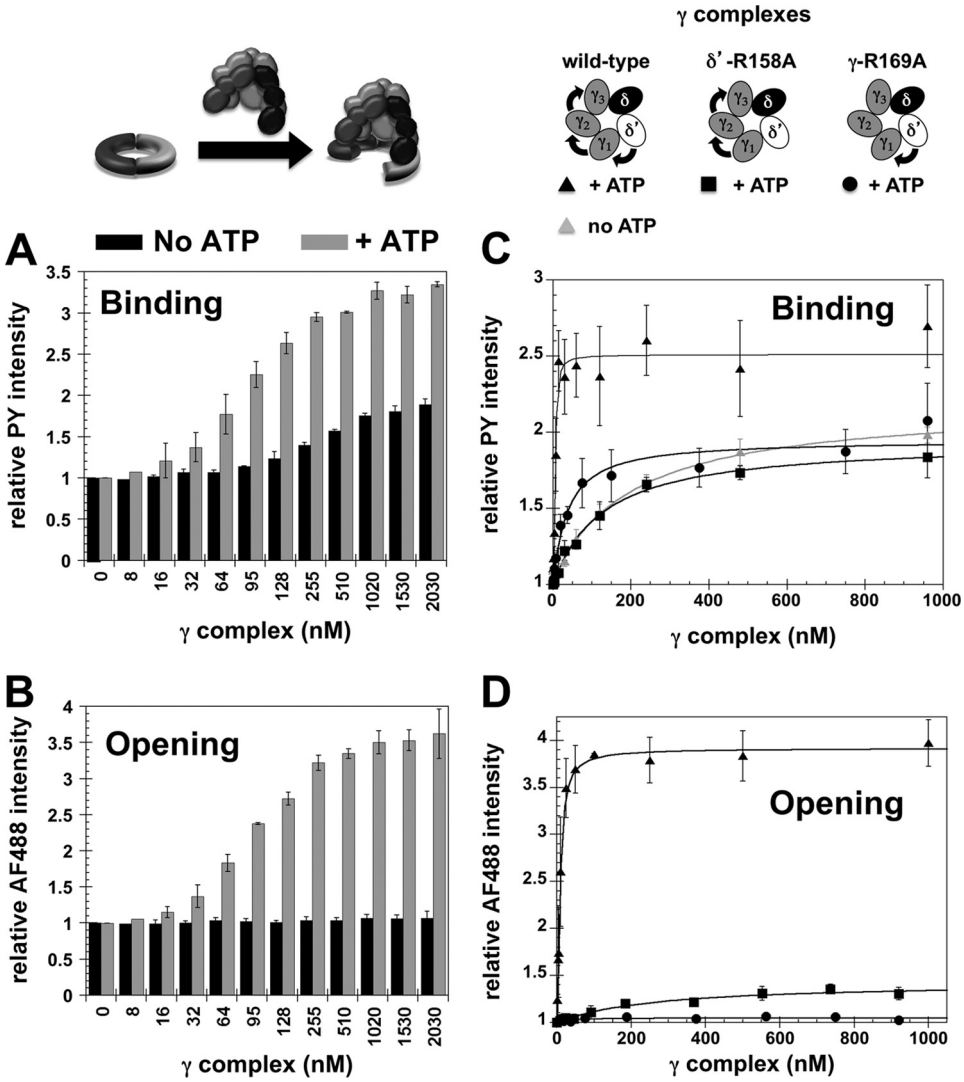

FIGURE 5. **Effects of ATP and arginine finger mutations on clamp binding and opening.** *A* and *B*, clamp binding and clamp opening in assays with 0.5 mM ATP (*gray bars*) and without ATP (*black bars*) were measured. The γ complex and ATP were added sequentially to solutions of 100 nM β-PY or 100 nM β-AF488$_2$ to measure clamp loader-clamp binding (*panel A*) and clamp opening (*panel B*), respectively. Relative intensities of PY at 375 nm and AF488 at 517 nm are plotted as a function of γ complex concentration. Intensities are relative to the values for solutions with no γ complex (0 nM γ complex). Average values from three independent experiments along with S.D. (*error bars*) are shown in each panel. *C* and *D*, wild-type γ complex contains three Arg fingers (illustrated by *curved arrows* in the scheme); one in the δ subunit that extends to the ATP site of the γ1 subunit, and one each in the γ1 and γ2 subunits that extend to the ATP sites of γ2 and γ3, respectively. Two γ complex mutants were made that contain either an Arg-158 to Ala in the δ′ subunit (δ′-R158A) or an Arg-169 to Ala in the γ subunits (γ-R169A) (21). Binding of γ-wt complex to β-PY was measured in the presence (*black triangles*) and absence (*gray triangles*) of 0.5 mM ATP, and binding of the δ′-R158A mutant (*squares*) and the γ-R169A mutant (*circles*) to β-PY were measured in the presence of 0.5 mM ATP (*panel C*). For each clamp loader, PY emission at 375 nm for the β-PY-clamp loader complex relative to free β-PY is plotted as a function of γ complex concentration for solutions containing 10 nM β-PY and 0.5 mM ATP (when present). Clamp opening (*panel D*) was measured for wild-type γ complex (*triangles*), the δ′-R158A mutant (*squares*), and the γ-R169A (*circles*) mutant in assays with 10, 2, and 5 nM β-AF488$_2$, respectively, and 0.5 mM ATP. For each clamp loader concentration, AF488 emission at 517 nm relative to free β-AF488$_2$ is plotted. Data shown are the average of three independent experiments.

binding sites, one in each of the γ subunits. Two of the three γ subunits extend an Arg finger to an adjacent ATP site and the δ′ subunit extends an Arg finger to the third ATP site. Because of this functional asymmetry, two different mutant clamp loaders can be made (Fig. 5); one containing a mutation to the Arg residue in the δ′ subunit (R158A) and another containing a mutation in the Arg residues in the γ subunits (R169A). These mutations do not affect ATP binding, and both clamp loaders bind three molecules of ATP, as does the wt clamp loader (21). The PY intensity-based assay was used to measure binding of the clamp loaders containing Arg finger mutations to β-PY under equilibrium conditions in assays containing 10 nM β-PY and 0.5 mM ATP. For comparison, binding of γ-wt complex to β-PY was measured in the presence (Fig. 5*C*, *black triangles*) and absence of ATP (Fig. 5*C*, *gray triangles*). There are two important results from these titrations of γ-wt complex. First, calculated dissociation constants, K_d values, were 0.9 ± 0.4 and 191 ± 44 nM in the presence and absence of ATP, respectively, showing that ATP increases the affinity of γ complex for β by at least 2 orders of magnitude. Second, at saturating concentrations of γ complex, the quantum yield of PY is lower in the absence of ATP than in the presence. Given that results in Fig. 5*B* showed that the clamp is not opened in the absence of ATP, this indicates that the PY fluorescence is lower in the closed clamp loader-clamp complex than in the open clamp loader-clamp complex. Binding of the Arg finger mutants to β-PY were

measured as for γ-wt complex but in the presence of ATP only Fig. 5*C*. Dissociation constants calculated from these titrations 124 ± 11 nM (*black squares*) and 28 ± 7 nM (*black circles*) for δ′-R158A and γ-R169A γ complexes, respectively. These K_d values are 138- and 31-fold greater than that for γ-wt complex, showing that the mutations greatly decrease the affinity of γ complex for β as previously reported (32). Additionally, at clamp loader concentrations in which β-PY binding was saturated by the mutant clamp loaders, the fluorescence intensity of PY was similar to that for the γ-wt complex in the absence of ATP where closed clamp loader-clamp complexes form. These data suggest that the mutant clamp loaders may have a defect in clamp opening.

To confirm that the Arg finger mutants have a defect in opening the β-clamp, equilibrium binding of γ complexes to β-AF488$_2$ was measured in assays containing 0.5 mM ATP (Fig. 5*D*). The mutant γ complex-δ′R158A gave only a 30–35% increase in AF488 fluorescence, and γ complex-γR169A gave no measurable increase in AF488 fluorescence at concentrations of 800–1000 nM clamp loader where binding approached saturation in Fig. 5*C*. Together, these results show that the Arg finger mutants are defective in clamp opening and that a defect in clamp opening may contribute to the decrease in affinity.

The γ Complex Actively Opens Clamps—Real-time clamp binding and opening measurements were made to determine how an open clamp loader-clamp complex forms. The γ complex could directly bind clamps that have transiently opened in solution, or the γ complex could bind closed clamps and actively open the clamps. To distinguish between these two alternatives, the rate of clamp binding was compared directly to the rate of clamp opening under identical conditions. If the γ complex were to directly bind clamps that have transiently opened in solution, then we would expect rates of binding and opening to be the same. However, if the γ complex were to bind a closed clamp and subsequently open the clamp, then we would expect the rate of opening to be slower than the rate of binding. To promote rapid binding, reactions contained a high concentration of γ complex (400 nM) relative to β-PY (20 nM) in binding assays or β-AF488$_2$ (20 nM) in opening assays. The increases in PY intensity (Fig. 6, *blue trace*) due to β binding and in AF488 intensity (Fig. 6, *black trace*) due to β opening are plotted on the same graph, so that rates can be directly compared. The results showed that the binding reaction is faster than the opening reaction, supporting the idea that the γ complex binds and then opens the β-clamp.

The argument could be made that the site-directed mutations and/or fluorophores introduced into the β clamps affect the interaction with the γ complex to give rise to this difference in rates. To rule out this possibility, a second kinetic approach was taken to establish that a two-step binding/opening reaction occurs. If the γ complex binds and then opens the clamp, then the rates of β opening should increase with γ complex concentration until the overall rate of the reaction becomes limited by the rate of clamp opening. Time courses for β opening were measured in assays containing 20 nM β-AF488$_2$ and 50–1600 nM γ complex (Fig. 7*A*). Fluorescence intensities for reaction time courses were normalized from 0 to 1 so that changes in amplitude with changes in γ complex concentration could

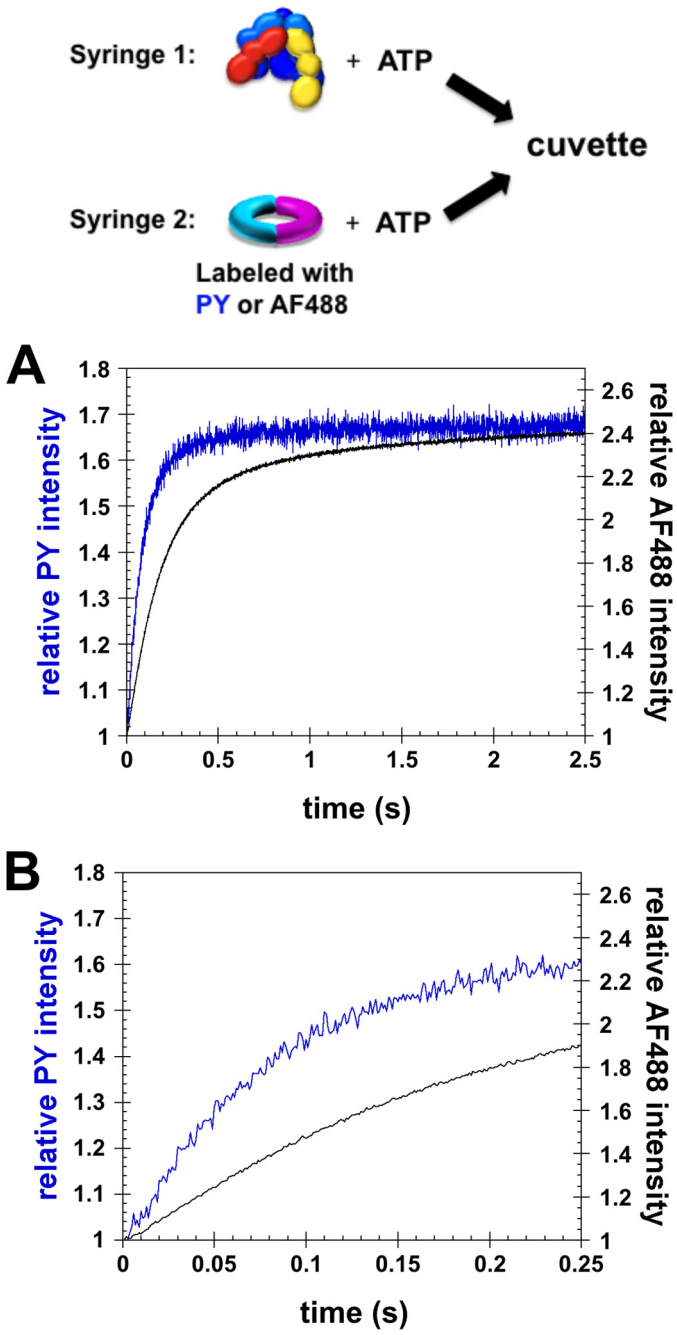

FIGURE 6. **Rates of clamp binding *versus* clamp opening.** *A*, stopped-flow fluorescence measurements were made in which a solution of γ complex and ATP was added to a solution of the β-clamp and ATP (see the mixing scheme). Final concentrations after mixing were 20 nM β, 400 nM γ complex, and 0.5 mM ATP. Clamp binding was measured using β-PY (*blue trace*) and clamp opening was measured using β-AF488$_2$ (*black trace*). The relative intensities of PY (*left axis*) and AF488 (*right axis*) are plotted on the same graph to highlight the relative timing of clamp binding and opening. *B*, the data from *panel A* are shown on a shorter time scale.

readily be evaluated. Time courses for reactions are not truly exponential but have sigmoidal character at early times as shown in the residuals to the fits (supplemental Fig. 2). However, these data were empirically fit to exponential rises ("Experimental Procedures," Equation 3) to get an estimate of the rates of change. Data were better fit by a double exponential than a single exponential (supplemental Fig. 2). The observed rate constants, k_{obs}, for both phases of the reactions

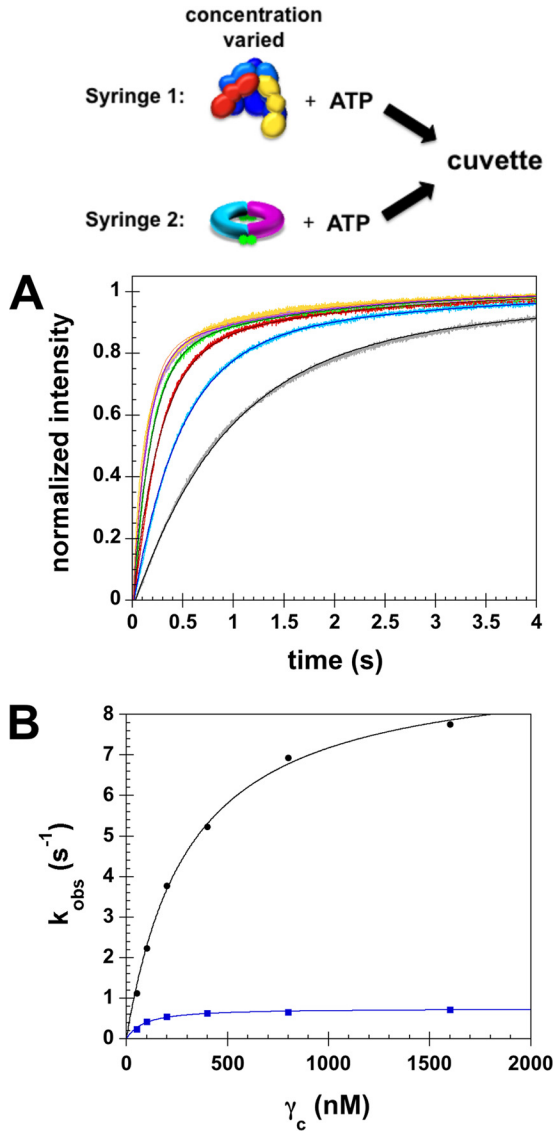

FIGURE 7. **Dependence of the clamp opening rate on the concentration of γ complex.** Rates of clamp opening as a function of γ complex concentration were measured by mixing solutions of γ complex and ATP with a solution of β-AF488$_2$ and ATP (see mixing scheme). *A*, time courses for opening reactions containing 50 (*gray*), 100 (*light blue*), 200 (*red*), 400 (*light green*), 800 (*purple*), or 1600 nM (*yellow*) γ complex and 20 nM β-AF488$_2$ are shown. Double exponential fits of the data are *solid lines* through reaction traces in darker shades of the same colors. *B*, data in *panel A* were fit to double exponential rises, and observed rate constants for both the fast (*black circles*) and slow (*blue squares*) phases of the reactions are plotted as a function of γ complex concentration. These data were globally fit to Equation 3 as described under "Experimental Procedures" (*solid lines*). Rate constants were allowed to vary with γ complex concentration, but amplitudes for the rapid and slow phases were fit to the same values for all six data sets. This fit yielded maximal rate constants of 9.3 and 0.75 s^{-1} for the fast and slow phases, respectively, and an amplitude of 0.83 for the rapid phase, 0.20 for the slow phase, and a constant of −0.03.

increased with increasing γ complex concentrations and approached maximal values (Fig. 7*B*). A maximal rate constant of about 9 s^{-1} for the rapid phase and about 0.8 s^{-1} for the slow phase of clamp opening was calculated by fitting the observed rate constants to Equation 4 ("Experimental Procedures"). The amplitudes of the fast and slow phases of the reactions were independent of the γ complex concentration, and a global fit of the time courses in Fig. 7*A* revealed that the amplitude of the rapid phase was ~80% of the total change in fluorescence. Possible mechanisms that give rise to the biphasic kinetics include a fraction of γ complex that is less reactive and gives a slower opening reaction or inhibition by a side reaction such as initial binding in an unproductive complex that can then dissociate and rebind to give a productive opening reaction.

DISCUSSION

Sliding clamps and clamp loaders are found among all domains of life. The *E. coli* proteins have served as a fundamental model system for investigating the mechanisms by which these proteins confer processivity to DNA polymerases and by which clamp loaders catalyze the mechanical clamp assembly reaction. In this work a clamp-opening assay was developed to facilitate mechanistic studies of the clamp loading reaction catalyzed by the *E. coli* clamp loader to determine the ATP requirements for clamp opening and the relative timing of clamp binding and clamp opening.

Our simple clamp-opening assay takes advantage of the property that fluorophores in close proximity will self-quench. When the β dimer is covalently labeled with AF488 on both sides of the monomer interfaces (Fig. 1), AF488 is quenched in the closed clamp, and this quenching is relieved to increase AF488 fluorescence when the clamp is opened. Control experiments demonstrated that introduction of mutations in the β-clamp to facilitate labeling and the fluorophores themselves did not adversely affect the structure of β or interactions with the γ complex. The relative intensity of AF488 provides a measure of the relative populations of clamps existing in an open or closed state under a given set of assay conditions. The observation that the relative intensity of β-AF488$_2$ bound by γ complex is about half that of β-AF488$_2$ denatured by SDS suggests that one interface of the clamp is opened and that most, if not, all of the clamp loader-clamp complexes exist in an open conformation.

ATP binding increases the affinity of γ complex for β and promotes β-clamp opening. ATP binding to the γ complex likely promotes a conformation that allows the individual subunits to productively bind and open the clamp. The γ and δ subunits alone are capable of opening clamps to unload them from circular DNA molecules, and the δ subunit can do so with about the same efficiency as the intact γ complex (5, 29, 33, 37). However, in clamp opening assays under equilibrium conditions, the δ subunit alone did not produce a measurable population of open clamps (data not shown). These two results are not necessarily in disagreement. To unload clamps from DNA, the δ subunit only needs to open the clamp transiently. Thus, only a small population of open clamps, which may not be observable in the AF488 opening assay, may be formed in solution. Alternatively, the δ subunit may interact with DNA, using it as a lever to gain torque for opening the clamp, and in this work, clamp opening by the δ subunit was measured in the absence of DNA.

By titrating β-AF488$_2$ with the γ complex or γ complex mutants, two types of information can be derived from the data. The γ complex concentration dependence of the increase in fluorescence provides a measure of the binding affinity, and the relative increase in AF488 fluorescence at saturating concen-

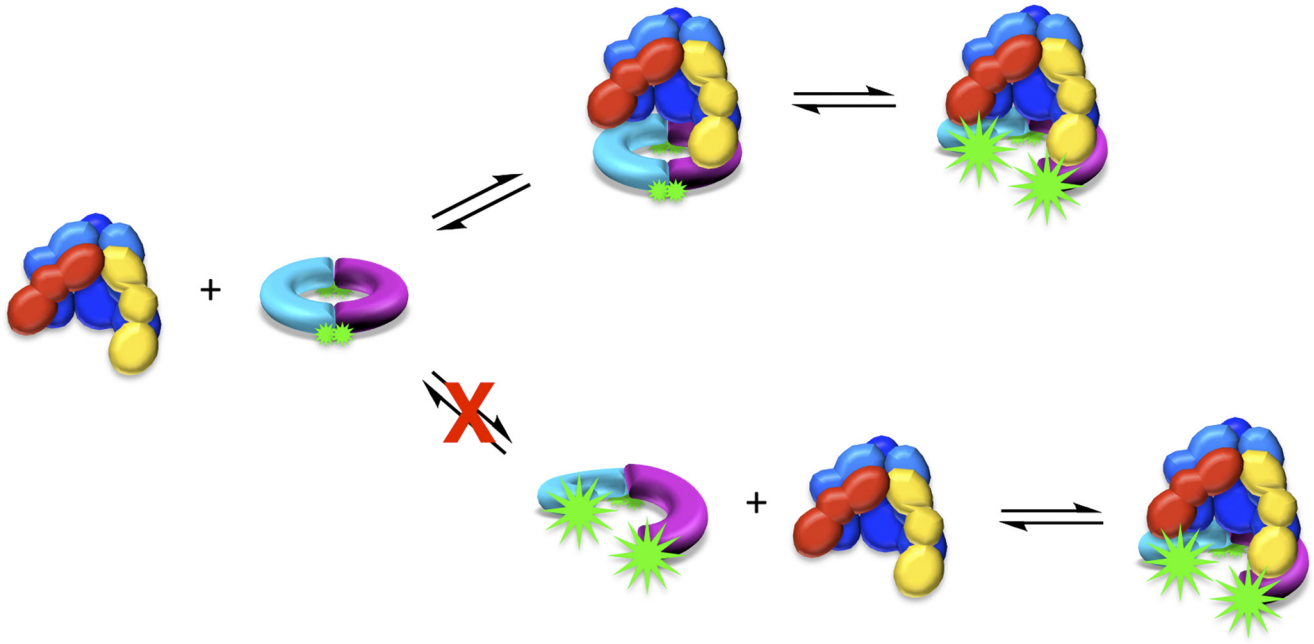

FIGURE 8. **The γ complex clamp loader actively opens the β-clamp.** Clamp loaders must hold sliding clamps in an open conformation to load the clamps onto DNA. This open clamp loader-clamp complex could form by a passive mechanism in which clamp loaders have a high affinity for clamps that have transiently opened in solution and passively capture clamps in this open conformation (*lower reaction pathway*). Alternatively, clamp loaders could bind closed clamps and actively pry them open. Data in Figs. 5 and 6 show that clamp binding is faster than clamp opening, demonstrating that the *E. coli* clamp loader actively opens the β-clamp after binding as illustrated in the upper reaction pathway rather than passively capturing clamps that have transiently opened.

trations of γ complex provides a measure of the fraction of clamps that are in an open conformation. In the absence of ATP, γ complex does not open the clamp even at high concentrations where the clamp is bound by γ complex (Fig. 5*B*). Interestingly in clamp binding and opening assays, Arg finger mutations cause the γ complex to behave as if they have a defect in ATP binding (Fig. 5, *C* and *D*). However, previous studies have shown that Arg finger mutants of γ complex bind three molecules of ATP, as does the wild-type clamp loader (21). Arginine fingers are part of a conserved sequence motif (for review, see Refs. 9–11 and 34)) that extends from one subunit to the γ-phosphate group of ATP bound to the adjacent subunit. This positioning can be seen in the recent crystal structure of the $\gamma_3\delta\delta'$ complex bound to ATP analog, ADP-BeF_3, and to primed template DNA (15). When the Arg fingers in either the δ′ subunit or in the γ subunits were converted to Ala, ATP-dependent clamp opening activity of the mutant clamp loaders was severely reduced (Fig. 5*D*). Based on the relative AF488 intensities at saturation, the δ′-R158A mutant produced about 16% of the open clamp loader-clamp complexes that the wild-type clamp loader formed, and the γ-R169A mutant produced less than 2% of the open complexes. This reduction in clamp opening activity was not due to a simple reduction in clamp binding activity because clamp opening was not observed at high concentrations of γ complex where clamp binding was nearly saturated (compare Figs. 5, *C* and *D*). Given that the Arg finger mutants are binding ATP (21), our results show that these mutants are not responding to bound ATP. This suggests that interactions between the Arg fingers and the γ-phosphates of the bound ATP molecules help to drive ATP-dependent conformational changes in the clamp loader that promote clamp opening. And conversely, loss of the Arg finger-γ-phosphate interactions upon hydrolysis of ATP may contribute to conformational changes that allow clamp closing and release. Interestingly, in a crystal structure of eukaryotic clamp loader, RFC, bound to PCNA, the PCNA clamp was in a closed conformation even though ATPγS was bound to RFC (38). In solution, ATPγS binding by both RFC and γ complex promotes formation of open clamp loader-clamp complexes (39, 40). Arg finger residues were mutated to Gln in RFC to help prevent ATP hydrolysis in the crystal. Our data would suggest that the reason that PCNA is not open in the structure is that RFC Arg finger mutants are also defective in clamp opening.

The key question addressed in this paper is how do open clamp loader-clamp complexes form (Fig. 8). Clamp loaders must either actively open closed clamps or capture clamps that have transiently and spontaneously opened. Studies show that the bacteriophage T4 clamp loader does the latter and preferentially binds open clamps to load them onto DNA (7, 8, 12–14). But the *E. coli* β-clamp and eukaryotic PCNA are more stable as closed rings than the bacteriophage T4 gp45 clamp. Both β and PCNA remain stably bound to circular DNA molecules for at least a half-hour, whereas the T4 clamp rapidly dissociates from DNA (5, 6). Given these differences, it is quite possible that a different mechanism of clamp opening is required to load β and PCNA onto DNA. Direct measurements of β-clamp binding and opening in solution show that clamp binding occurs before clamp opening (Fig. 6). This timing of events shows that the γ complex binds closed clamps in solution before opening the clamps. This two-step opening reaction was confirmed in experiments measuring the γ complex concentration dependence of clamp opening (Fig. 7) in which clamp opening rates approached a maximal value with increasing γ complex concentrations. These kinetics of β-clamp open-

ing are consistent with previously measured kinetics of β-clamp binding where an apparent bimolecular rate constant of 2.3×10^7 $M^{-1}s^{-1}$ was determined (22). At the two lowest γ complex concentrations, 50 and 100 nM, in Fig. 7*B*, the opening rate is dominated by the binding rate, and the observed rate constants are the same as those calculated from the bimolecular rate constant for binding and γ complex concentrations. At higher γ complex concentrations, the rate constant for opening starts to contribute to the observed rate, and the plot of observed rates *versus* γ complex concentration no longer increases linearly with concentration approaching a maximum value of about 9 s^{-1}.

PCNA opening has been measured in a FRET-based assay to determine the distance that a monomer interface opens in a complex with RFC (41). A rate of formation of an open RFC-PCNA complex of 2.1 s^{-1} was determined, and given that this rate did not change when the concentration of RFC was reduced by a factor of two, this suggests that RFC may also actively open PCNA. Assuming that this is the case, a comparison of the opening rates shows that the γ complex opens β about 4–5 times faster than RFC opens PCNA. This is somewhat surprising given that the β ring appears to be more stable than PCNA as assessed by the dissociation constants to produce monomers and the lifetimes of the rings on circular DNA molecules (6). It is possible that the γ complex is a more efficient clamp opener than RFC. A faster more efficient opening reaction may be required for clamp loading on the lagging strand in *E. coli* because the *E. coli* replication fork moves about 10 times faster than the eukaryotic fork.

In summary, a simple assay for measuring β-clamp opening and closing was developed. Using this assay along with a clamp binding assay, the first evidence that *E. coli* clamp loaders may actively pry clamps open to load clamps onto DNA was obtained. The combination of real-time clamp binding and opening assays will serve as excellent tools for future experiments aimed at defining mechanistic requirements for clamp loading and for determining the relative timing of individual events in the clamp loading reaction cycle.

REFERENCES

1. Gulbis, J. M., Kelman, Z., Hurwitz, J., O'Donnell, M., and Kuriyan, J. (1996) *Cell* **87,** 297–306
2. Kong, X. P., Onrust, R., O'Donnell, M., and Kuriyan, J. (1992) *Cell* **69,** 425–437
3. Moarefi, I., Jeruzalmi, D., Turner, J., O'Donnell, M., and Kuriyan, J. (2000) *J. Mol. Biol.* **296,** 1215–1223
4. Shamoo, Y., and Steitz, T. A. (1999) *Cell* **99,** 155–166
5. Leu, F. P., Hingorani, M. M., Turner, J., and O'Donnell, M. (2000) *J. Biol. Chem.* **275,** 34609–34618
6. Yao, N., Turner, J., Kelman, Z., Stukenberg, P. T., Dean, F., Shechter, D., Pan, Z. Q., Hurwitz, J., and O'Donnell, M. (1996) *Genes to Cells* **1,** 101–113
7. Alley, S. C., Shier, V. K., Abel-Santos, E., Sexton, D. J., Soumillion, P., and Benkovic, S. J. (1999) *Biochemistry* **38,** 7696–7709
8. Millar, D., Trakselis, M. A., and Benkovic, S. J. (2004) *Biochemistry* **43,** 12723–12727
9. Erzberger, J. P., and Berger, J. M. (2006) *Annu. Rev. Biophys. Biomol Struct.* **35,** 93–114
10. O'Donnell, M., and Kuriyan, J. (2006) *Curr. Opin. Struct. Biol.* **16,** 35–41
11. White, S. R., and Lauring, B. (2007) *Traffic* **8,** 1657–1667
12. Alley, S. C., Abel-Santos, E., and Benkovic, S. J. (2000) *Biochemistry* **39,** 3076–3090
13. Trakselis, M. A., Alley, S. C., Abel-Santos, E., and Benkovic, S. J. (2001) *Proc. Natl. Acad. Sci. U.S.A.* **98,** 8368–8375
14. Zhuang, Z., Berdis, A. J., and Benkovic, S. J. (2006) *Biochemistry* **45,** 7976–7989
15. Simonetta, K. R., Kazmirski, S. L., Goedken, E. R., Cantor, A. J., Kelch, B. A., McNally, R., Seyedin, S. N., Makino, D. L., O'Donnell, M., and Kuriyan, J. (2009) *Cell* **137,** 659–671
16. Anderson, S. G., Thompson, J. A., Paschall, C. O., O'Donnell, M., and Bloom, L. B. (2009) *Biochemistry* **48,** 8516–8527
17. Dong, Z., Onrust, R., Skangalis, M., and O'Donnell, M. (1993) *J. Biol. Chem.* **268,** 11758–11765
18. Maki, S., and Kornberg, A. (1988) *J. Biol. Chem.* **263,** 6547–6554
19. Olson, M. W., Dallmann, H. G., and McHenry, C. S. (1995) *J. Biol. Chem.* **270,** 29570–29577
20. Onrust, R., Finkelstein, J., Naktinis, V., Turner, J., Fang, L., and O'Donnell, M. (1995) *J. Biol. Chem.* **270,** 13348–13357
21. Johnson, A., and O'Donnell, M. (2003) *J. Biol. Chem.* **278,** 14406–14413
22. Thompson, J. A., Paschall, C. O., O'Donnell, M., and Bloom, L. B. (2009) *J. Biol. Chem.* **284,** 32147–32157
23. Johanson, K. O., Haynes, T. E., and McHenry, C. S. (1986) *J. Biol. Chem.* **261,** 11460–11465
24. Oakley, A. J., Prosselkov, P., Wijffels, G., Beck, J. L., Wilce, M. C., and Dixon, N. E. (2003) *Acta Crystallogr D. Biol. Crystallogr.* **59,** 1192–1199
25. Otwinowski, Z., and Minor, W. (1997) *Processing of X-ray Diffraction Data Collected in Oscillation Mode*, Elsevier, Inc., Amsterdam
26. Adams, P. D., Grosse-Kunstleve, R. W., Hung, L. W., Ioerger, T. R., McCoy, A. J., Moriarty, N. W., Read, R. J., Sacchettini, J. C., Sauter, N. K., and Terwilliger, T. C. (2002) *Acta Crystallogr. D. Biol. Crystallogr.* **58,** 1948–1954
27. Emsley, P., and Cowtan, K. (2004) *Acta Crystallogr. D. Biol. Crystallogr.* **60,** 2126–2132
28. Laskowski, R. A., MacArthur, M. W., Moss, D. S., and Thornton, J. M. (1993) *J. Appl. Crystallogr.* **26,** 283–291
29. Turner, J., Hingorani, M. M., Kelman, Z., and O'Donnell, M. (1999) *EMBO J.* **18,** 771–783
30. Naktinis, V., Onrust, R., Fang, L., and O'Donnell, M. (1995) *J. Biol. Chem.* **270,** 13358–13365
31. Hingorani, M. M., Bloom, L. B., Goodman, M. F., and O'Donnell, M. (1999) *EMBO J.* **18,** 5131–5144
32. Snyder, A. K., Williams, C. R., Johnson, A., O'Donnell, M., and Bloom, L. B. (2004) *J. Biol. Chem.* **279,** 4386–4393
33. Stewart, J., Hingorani, M. M., Kelman, Z., and O'Donnell, M. (2001) *J. Biol. Chem.* **276,** 19182–19189
34. Ogura, T., Whiteheart, S. W., and Wilkinson, A. J. (2004) *J. Struct. Biol.* **146,** 106–112
35. Karata, K., Inagawa, T., Wilkinson, A. J., Tatsuta, T., and Ogura, T. (1999) *J. Biol. Chem.* **274,** 26225–26232
36. Johnson, A., Yao, N. Y., Bowman, G. D., Kuriyan, J., and O'Donnell, M. (2006) *J. Biol. Chem.* **281,** 35531–35543
37. Leu, F. P., and O'Donnell, M. (2001) *J. Biol. Chem.* **276,** 47185–47194
38. Bowman, G. D., O'Donnell, M., and Kuriyan, J. (2004) *Nature* **429,** 724–730
39. Gomes, X. V., and Burgers, P. M. (2001) *J. Biol. Chem.* **276,** 34768–34775
40. Hingorani, M. M., and O'Donnell, M. (1998) *J. Biol. Chem.* **273,** 24550–24563
41. Zhuang, Z., Yoder, B. L., Burgers, P. M., and Benkovic, S. J. (2006) *Proc. Natl. Acad. Sci. U.S.A.* **103,** 2546–2551